

Influence of target area density parameter and electrostatic pulse width modulation variable nozzle on physical characteristics of precision spray

Zhen Lin^{1*}, Shengkai Liang¹, Jinye Xie¹, and Shuo Tian¹

¹University of Sanya, 191 Xueyuan Road, Jiyang District, 572022, Sanya City, Hainan Province, China.

Abstract. This paper discusses the observation of different precision spraying processes of pulse width modulated variable sprinkler in electrostatic field under different target area densities and discusses the physical characteristics of precision spraying under electrostatic action of different target area density parameters and pulse width modulated variable sprinkler, the influence of various parameters of precision spraying on spray settling rate. Using different environmental protection liquid, the point cloud density detected by the laser Light Detection and Ranging (LiDAR) sensor was used to test different targets and obtain the physical parameter of area density. The area density of the target was differentiated and classified. According to the area density of the target of different categories, multi-directional research was carried out with the conductivity of the liquid itself and the charge rate of the liquid itself under the action of the electrostatic pulse width modulation variable nozzle. The relationship between the three was studied, and a good spray control strategy was obtained. When the area density was 0.668, the conductivity was 10.0 mS/cm, and the spray pressure was 0.45MPa, the charge-mass ratio was the largest and the deposition effect was the best, this paper studies the improvement of the environment and the sustainable development of pesticide use in the future.

1 Introduction

This paper proposes to first test different targets and obtain area density through the point cloud density detected by laser LiDAR sensor. Then, the obtained morphological parameters such as canopy volume and area can reflect the canopy characteristics and plant health degree of plants, and the morphological parameters detected by LiDAR sensor can also be used to evaluate plant health according to different plant targets. The corresponding plant target morphological parameters were obtained, and the precise spray parameters were adjusted according to the morphological parameters. According to the principle of precision agriculture, PWM allows the required amount of spray to be sprayed where needed, without changing the droplet size spectrum, which helps to improve the uniformity of spray quality

*Corresponding author: 2257560314@qq.com

and reduce droplet drift and diffusion [1]. In contrast, this paper obtains the corresponding target plant morphological parameters, and adjusts the precise spray parameters according to the morphological parameters. The program will be used for pesticide spraying operations in agricultural fields. Its design and function are designed to improve the efficiency, accuracy and safety of pesticide spraying, reduce the labor burden of farmers, and reduce the negative impact on the environment. These data can be used for crop growth analysis, early warning of pests and diseases, and optimization of agricultural decisions to promote the development of intelligent agriculture and improve the scientific and efficiency of agricultural production, achieve green and sustainable development of precision spray application.

2 Materials and methods

2.1 Experimental platform

2.1.1 Hardware construction

The test platform is composed of hardware and software, as shown in the figure. In order to ensure that the mobile robot has good traffic capacity, the robot belt bottom plate is driven by a servo motor, which can directly control the linear speed and angular speed of the two-track driving wheel. The Lidar local coordinate system XOY meets the right-handed rule, taking the geometric center of 3DLiDAR as the coordinate origin O, the forward direction of the robot is the positive direction of the X-axis, the vertical X-axis to the left is the positive direction of the Y-axis, and the Z-axis is determined by the right-handed rule. Hardware selection of laser radar, microcomputer, equipped with i7-5820k processor, 32G memory, 256G solid state disk and Ubuntu18.04 as the operating system of the industrial computer, using 12V, 5000mA aircraft model lithium battery for the sensor and industrial computer power supply. The equipment diagram is shown in Figure 1(a), and the target site is shown in Figure 1.



Fig. 1. Equipment and target map.

2.1.2 LiDAR point cloud processing framework

The software required to deal with point cloud is deployed in the open-source robot operating system (ROS), C++ and Python are used as the opening language of the system, and Tensorflow is used as the deep learning framework for the development of point cloud recognition algorithms. The collected target data was transmitted to the back-end laboratory workstation for global point cloud identification and canopy measurement, as shown in Figure 2.

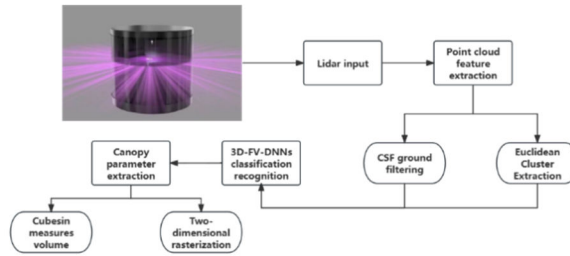
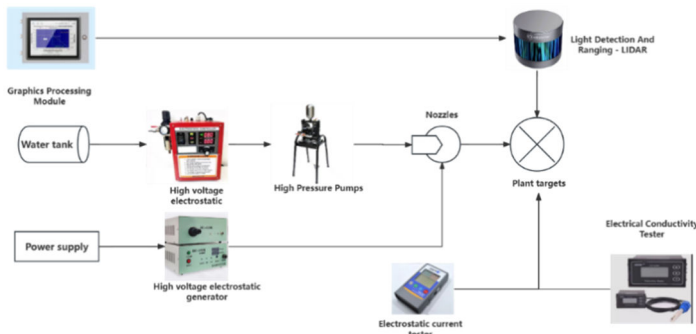


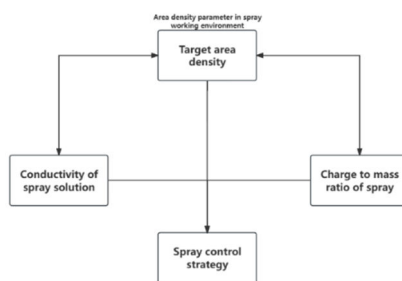
Fig.2. Point cloud identification and detailed canopy extraction process.

2.1.3 Test system idea

According to the surrounding environment of the laser LiDAR scanning test, different area density parameters were obtained at different locations, and the conductivity and charge-mass ratio of the liquid under the action of the electrostatic pulse width modulated variable nozzle were measured at the same time. Combined with the relationship between the three, the precise spray control strategy was obtained according to the comparative iterative training. The test flow chart is shown in Figure 3(a), and the control strategy idea diagram is shown in Figure 3(b).



(a)



(b)

Fig. 3. Test flow chart and control strategy diagram.

2.2 Liquid test

2.2.1 Measurement of electrical conductivity and charge-mass ratio of spray liquid under variable pulse width modulation nozzle

(1) Measurement of electrical conductivity of liquid medicine

The measurement of the solution conductivity requires two parameters: the conductivity G of the solution and the geometric parameter c of the electrode. The conductivity can be obtained by measuring the current and voltage according to the formula, and then the conductivity can be obtained by using the geometric parameter of the electrode according to the formula in Equation (1), as follows:

$$\kappa = \frac{1}{A} * G = c * G \quad (1)$$

Where $c = L/A$, unit cm^{-1} ; A is the effective cross-sectional area of the measuring electrode; l is the distance between the two plates; c is the electrode constant. In the presence of a uniform electric field between the electrodes, the electrode constant can be calculated from the geometry [2].

The measurement of electrical conductivity usually uses an electrical conductivity meter, which is a common instrument used to measure the electrical conductivity of electrolyte solutions. The conductivity meter usually applies a stable AC electrical signal between the electrodes of the conductivity cell to prevent serious errors caused by the phenomenon of "polarization". By measuring the solution conductance between the electrodes, the conductivity is obtained according to the determined conductivity cell constant.

(2) Measurement of charge to mass ratio with liquid medicine

At present, domestic and foreign research on static electricity mainly focus on the improvement of electrostatic spray equipment and the research and development of new electrostatic spray equipment. In 2014, Zhang Ling et al. designed a new type of electrostatic nozzle and measured the charging effect of the nozzle with a charge-to-mass ratio measuring device [3]. In 2003, G N Laryea et al. developed a new type of electrostatic pressure swirl nozzle and tested its spray characteristics [3]. Weighing technology was adopted in the measurement of spray loss, overcoming the difficulties of traditional loss measurement. The test results show that the use of electrostatic technology can improve the deposition of plant canopy, and the test system diagram is shown in Figure 4.

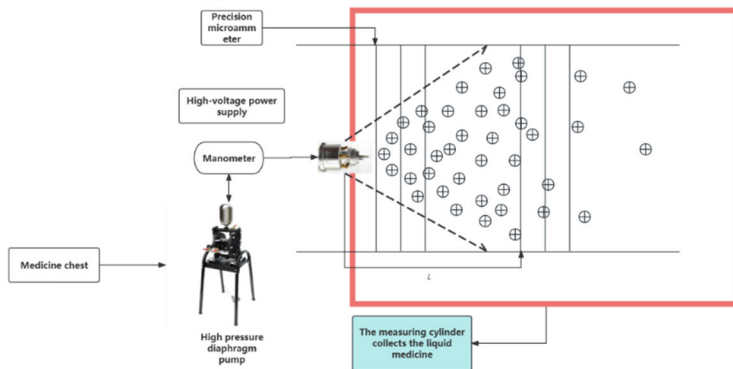


Fig. 4. Charge-mass ratio measuring device diagram.

3 Test results and analysis

3.1 Canopy parameter measurement test

In order to verify the accuracy of canopy reconstruction, canopy volume and area, these parameters were measured manually as the real values of the test and compared with the measured values of the system, and the determination coefficient R^2 and mean square root error RMSE were used as the evaluation criteria. 40 seedling nurseries were randomly selected from the sample as test samples, and their R^2 and RMSE were counted. The statistical results are shown in Figure 5.

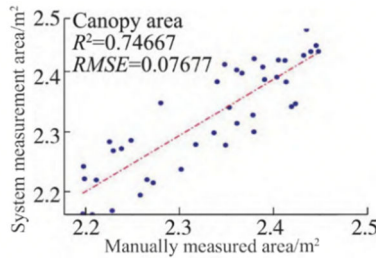


Fig. 5. Plot of canopy statistics.

For nurseries whose canopy shapes are similar to ellipsoids and cones, the corresponding formula can be used to calculate the canopy volume and area. However, due to the random sampling method, the measured canopy parameters of some plants whose canopy shapes are not ellipsoids or cones still differ from those of the system parameters. It can be seen from Figure 5 that the R^2 and RMSE values measured by canopy volume are 0.6978 and 0.09754, and the R^2 and RMSE values measured by canopy area are 0.7467 and 0.07677. It shows that the canopy parameter values obtained in this paper are highly correlated and effective with those measured manually.

3.2 Single factor comparison test of electrical conductivity and charge-mass ratio of spray solution with target area density

3.2.1 The influence of different electrical conductivity of spray liquid and different target area density on deposition rate under pulse width modulated variable spray nozzle

The test area density parameters were taken with the previous test set and the spray pressure was set at 0.4Mpa. When the conductivity is 0.3mS/cm, it is commonly used tap water. NaCl is added to tap water to change the solution conductivity. It can be seen from Figure 6 that under the condition of the same area density [5], the droplet charge-mass ratio increases with the increase of the solution conductivity, and reaches the maximum when the conductivity is 10.089 mS/cm. This situation can be explained by the droplet formation time, according to the formula of the charging time constant: $T_c = S/\epsilon$ (S is the conductivity, ϵ is the dielectric coefficient of the solution), and the solution conductivity and the charging time constant T_c is inversely proportional. NaCl dissolved in the solution may lead to changes in solution viscosity, surface tension, etc, thus affecting the droplet size and thus the charge-mass ratio, thus affecting the deposition effect. In other words, under the working environment of area density with determination coefficient of 0.66, the optimal state is reached when the

conductivity is 10.0 mS/cm, and the increase of conductivity or area density can no longer improve the deposition effect.

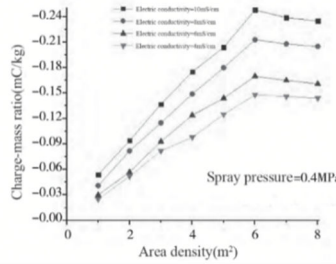


Fig. 6. Area density parameter and conductivity test diagram.

3.2.2 The effects of different charge to mass ratio and different target area density on deposition rate were investigated under the pulse width modulated variable spray nozzle

The effects of different charge to mass ratio and different target area density on deposition rate were investigated under the pulse width modulated variable spray nozzle. The test set the spray pressure at 0.4MPa and the conductivity at 10.0mS/cm. The results (Figure 7) show that under the condition of the same area density, the droplet charge-mass ratio increases with the decrease of the nozzle aperture. Under pressure, the liquid is sprayed out of the nozzle at a very high speed into the static or low speed air flow, breaking through the resistance to form small droplets. According to Bernoulli's principle [6], when the area density remains unchanged, the smaller the aperture, the larger the flow velocity, and the smaller the particle size of the droplets formed. In addition, due to the Rayleigh limit [7], the amount of charge charged by the droplets is inversely proportional to the particle size of the droplets. Therefore, under the same spray conditions, the larger the nozzle aperture, the lower the droplet charge to mass ratio. Therefore, the preliminary conclusion is drawn that when the area density is 0.668, the conductivity is 10.0 mS/cm, and the spray pressure is 0.45MPa. The maximum charge-mass ratio has the best deposition effect.

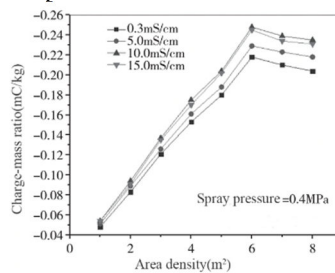


Fig. 7. Area density parameter and charge-mass ratio test diagram.

4 Conclusion

The following conclusions are drawn: (1) Under single factor conditions, the charge-mass ratio decreases with the increase of nozzle aperture and increases with the increase of area density; In a certain range of target area density, the ratio of charge to mass increased with the increase of conductivity, reached the maximum at 10.0 mS/cm, and then decreased with the increase of conductivity. In a certain range, the ratio of charge to mass increased with the increase of plant target area density, reached the maximum at 6 kV, and then decreased with

the increase of plant target area density [8]. (2) When the area density is 0.668, the conductivity is 10.0 mS/cm, and the spray pressure is 0.45MPa, the charge-mass ratio is the largest and the deposition effect is the best. The error is small, and the parameters are reliable. At the same time, this experiment also provides a way to optimize the analysis of more than 3 influencing factors [9]. In this paper, by studying the effects of target area density parameters and electrostatic pulse width modulation variable nozzles on the physical characteristics of precision spray, we can get a novel method to improve the adhesion rate of droplets to plants and achieved green and sustainable development of precision spray application. However, due to the limited range of the pressure gauge, the limit value of the droplets under pressure is not found in this test, which needs further study.

References

1. M. Grella, F. Gioelli, P. Marucco, I. Zwervaegher, E. Mozzanini, N. Mylonas, D. Nuyttens, P. Balsari, Field assessment of a pulse width modulation (PWM) spray system applying different spray volumes: duty cycle and forward speed effects on vines spray coverage. *Precis. Agric.* **23**, 219–252 (2022).
<https://doi.org/10.1007/s11119-021-09835-6>
2. W. Liu, X. He, Y. Liu, Z. Wu, C. Yuan, L. Liu, P. Qi, T. Li. Navigation method between rows for orchard based on 3DLiDAR. *Trans. Chin. Soc. J. Agric. Agric. Eng.*, **37** (9), 165-174 (2021). <https://doi.org/10.11975/j.issn.1002-6819.2021.09.019>
3. N. Bao, S. Zhang, X. Mo. Overview of tree crown structure. *Eucalyptus Science and technology Technology*, **38**(1), 68-74 (2021).
<https://doi.org/10.13987/j.cnki.askj.2021.01.012>
4. L. Zhang, X. Xue, Z. Sun, S. Zhang, C. Chen, Optimal design and experiment of electrostatic electrode for conical fog nozzle. *China Agric.Chin. J. Mech. Chem*, **35**(04), 128-131 (2014). <https://doi.org/10.13733/j.jcam.issn.2095-5553.2014.04.032>
5. G. N. Laryea, S. No, Development of electrostatic pressure-swirl nozzle for agricultural applications. *J. Electrostat.*, **57**, 129-142 (2003).
[https://doi.org/10.1016/S0304-3886\(02\)00122-5](https://doi.org/10.1016/S0304-3886(02)00122-5)
6. J.P. Skovsgaard, O. Clémentine, M.C. Rebecka, High-pruning of silver birch (*Betula pendula* Roth): work efficiency as a function of pruning method, pole saw type, slash removal, operator, pruning height and branch characteristics. *Scand. J. For. Res.*, **33**(5), 511-517 (2018). <https://doi.org/10.1080/14942119.2018.1462593>
7. K. Stühm, A. Tornow, J. Schmitt, L.Grunau, F. Dietrich, K.Dröder, A novel gripper for battery electrodes based on the Bernoulli principle with integrated exhaust air compensation, *Proc. CIRP*, **23**, 161-164 (2014).
<https://doi.org/10.1016/j.procir.2014.10.065>
8. H. Franklin, Rayleigh limits for effective wavenumbers of randomly distributed porous cylinders. Comparison of explicit and implicit methods, *Wave Motion*, **66**, 106-117 (2016). <https://doi.org/10.1016/j.wavemoti.2016.06.005>
9. M. Karkee, B. Adhikari, S. Amatya, Q. Zhang, Identification of pruning branches in tall spindle apple trees for automated pruning, *Comput. Electron. Agric.*, **103**, 127-135 (2014). <https://doi.org/10.1016/j.compag.2014.02.013>